GEMINI/GMOS SEARCH FOR MASSIVE BINARIES IN THE IONIZING CLUSTER OF 30 DOR

Guillermo Bosch[1,3], Elena Terlevich[2], and Roberto Terlevich[2]
[1] Facultad de Ciencias Astronómicas y Geofísicas, Paseo del Bosque s/n, 1900 La Plata, Argentina; guille@fcaglp.unlp.edu.ar
[2] INAOE, Tonantzintla, Apdo. Postal 51, 72000 Puebla, Mexico

ABSTRACT

If binaries are common among massive stars, it will have important consequences for the derivation of fundamental properties such as the cluster age, initial mass function, and dynamical mass. Making use of the multiplexing facilities of the Gemini Multi-Object Spectrograph, we were able to investigate the presence of binary stars within the ionizing cluster of 30 Doradus. From a seven-epoch observing campaign at Gemini South we detect a binary candidate rate of about 50%, which is consistent with an intrinsic 100% binary rate among massive stars. We find that single-epoch determinations of the velocity dispersion give values around 30 km s^{-1}. After correcting the global velocity dispersion for the binary orbital motions, the "true" cluster velocity dispersion is 8.3 km s^{-1}. This value implies a virial mass of about 4.5×10^5 $M_\odot$ or 8% of the mass calculated using the single-epoch value. The binary corrected virial mass estimate is consistent with photometric mass determinations, thus suggesting that NGC 2070 is a firm candidate for a future globular cluster.

Key words: binaries: spectroscopic – galaxies: clusters: general – Magellanic Clouds – stars: early-type – stars: kinematics

1. INTRODUCTION

30 Doradus in the Large Magellanic Cloud (LMC) is the nearest available example of a young and massive starburst cluster. Given its proximity it is possible to perform a highly detailed study of its stellar component. The large number of massive stars present in this single cluster allows the statistical analysis of several parameters at a level of significance that is not available in the local and smaller Galactic clusters.

Although a large amount of work has been devoted to the study of the 30 Dor ionizing cluster, some important topics, such as the binary fraction among its massive stars, remain relatively unexplored. If binaries are common among massive stars, it will have important consequences for the derivation of fundamental properties such as the cluster age, initial mass function (IMF), and dynamical mass. In particular, the orbital motions of massive binary stars in a young stellar cluster can have a large impact on the measurement of its global stellar velocity dispersion and, consequently, on the dynamical mass determination.

Bosch (1999) and collaborators pointed out that the observed radial velocity dispersion of stars within the cluster can be strongly affected by the orbital motions of massive binaries. Single-epoch mid-resolution spectra obtained at ESO with the New Technology Telescope (NTT; Bosch et al. 1999) were used to perform a radial velocity analysis on the stars that conform to the ionizing cluster of 30 Dor (Bosch et al. 2001). The most important results of that analysis can be outlined as follows:

1. A high value of the velocity dispersion ($\sigma \sim 35$ km s^{-1}) was obtained for the OB stars within NGC 2070, the ionizing cluster in 30 Dor.

2. Estimates of the influence that an underlying binary population could have on this determination revealed that orbital motion within the binary pair could mimic this large velocity dispersion.

3. From the photometric mass of 30 Dor a rather uncertain value for the virial motions was estimated to be around 10 km s^{-1}.

Although these results are consistent with a 100% binary population, it is necessary to confirm this assumption with direct evidence. The issue of binary frequency is still subject to debate, as most of the statistics on binary stars are biased toward later type stars (Lada 2006). There is evidence pointing toward a relatively high number of binaries among early-type stars (Mason et al. 1998), but previous studies based on single Galactic clusters using similar techniques (such as Sana et al. 2008) deal with a smaller number of stars, each of them observed on different numbers of epochs.

Here we present a new set of observations of NGC 2070 obtained with the Gemini Multi-Object Spectrograph (GMOS) at Gemini South. These comprise multiobject optical spectroscopy of 50 early-type stars observed at least in six different epochs. The aim is to detect spectroscopic binary stars from variations in their radial velocities.

2. OBSERVATIONS AND DATA REDUCTION

Observations were performed at the Gemini South Observatory (proposals GS-2005B-Q-2 and GS-2006B-Q-21) using two multislit masks. Targets within each mask were selected from a previous imaging run with the GMOS according to their spectral types as determined and compiled in Bosch et al. (1999). Spectra were obtained during nights of 2005 September and 2005 December for the first run, and 2006 December and 2007 January for the second run. Approximate HJD for the listed observations are shown in Table 1. The instrument was set up with the B1200 grating R $\sim$ 3700 centered at about 4500 Å, which yields a resolution of 0.25 Å per pixel at the CCD. Although the wavelength range varies slightly in MOS spectroscopy, the region from 3900 Å to 5500 Å is covered by our spectra. The total integration time was split in three to allow for the wavelength dithering pattern needed to cover the gaps between GMOS CCDs. Overall signal-to-noise ratios (S/Ns) are above 150. These ratios are measured on reduced spectra,

---

[3] IALP, UNLP-CONICET, Argentina.

Table 1
Log of Observations

Observing Date	MaskI	MaskII
2005 Sep 7	2453620.89	
2005 Dec 19		2453723.58
2005 Dec 20	2453724.58	
2005 Dec 22		2453726.68
2005 Dec 23	2453727.65	
2005 Dec 24		2453728.59
2006 Nov 29	2454068.73	
2006 Nov 30		2454069.70
2006 Dec 24	2454093.83	
2006 Dec 31		2454100.86
2007 Jan 1	2454101.79	2454101.73
2007 Jan 9		2454109.66

Note. Observing dates are listed in Column 1 and Heliocentric Julian dates for masks I and II are shown in Columns 2 and 3, respectively.

dividing the average value of the stellar continuum by the scatter over the same spectral range. No flux calibration stars were observed as they were not needed for our purposes.

Data were reduced following standard procedures, using the GMOS reduction tasks within the Gemini IRAF[4] package.

3. RADIAL VELOCITIES

3.1. Zero-Point Errors

We were able to check for the presence of zero-point errors in our radial velocity determinations using the nebular lines present throughout the region. Nebular spectra were wavelength calibrated together with the stellar spectra so as to provide a strong template to check for variations of our radial velocities' zero point at different epochs. Nebular emission lines have strong narrow profiles, enabling us to cross-correlate nebular spectra obtained on different nights using fxcor within IRAF, which yields accurate determinations of radial velocity differences, if present. Radial velocities derived for each night (V_{neb}) are very stable when observations on different epochs are compared and their variations $|\Delta V_{neb}|$ were found to be negligible ($|\Delta V_{neb}| \leqslant 1.0$ km s^{-1}, $\sigma_{neb} = 3.1$ km s^{-1}), which suggests that there is no systematic shift introducing spurious variations of stellar radial velocities between epochs.

3.2. Measurements

Radial velocities were derived measuring absorption line profiles with the aid of the ngaussfit task within the STSDAS/IRAF package, following a procedure similar to that described in Bosch et al. (2001). This allowed us to derive individual radial velocities for each spectral line, and handle each element (or each ion in the case of He) separately. Stellar radial velocities were derived using the best set of lines available, according to the star's spectral type. Although this means that we are not using the same set of lines for the whole sample, we strictly kept the same set of lines for the same star on different epochs when looking for radial velocity variations. Uncertainties introduced when fitting individual Gaussians to the absorption profiles are of the order of 5 km s^{-1}.

---

[4] IRAF is distributed by the National Optical Astronomy Observatories, which are operated by the Association of Universities for Research in Astronomy, Inc., under cooperative agreement with the National Science Foundation.

Table 2 lists the complete set of radial velocities determined for the sample stars. Stars are labeled following the nomenclature of Parker (1993) and data columns include average radial velocity (and its uncertainty) for each epoch. The errors listed in Columns 3, 5, 7, 9, 11, 13, and 15 in Table 2 correspond to the internal error σ_I, which is the quadratic sum of the standard deviation of the estimated average from the set of available lines and the minimum uncertainty (3.1 km s^{-1}) as derived from high S/N narrow nebular emission lines. Column 16 shows the ratio between the standard deviation of stellar radial velocity between different epochs and the average of σ_I. Spectral types are given for reference in Column 2.

4. RESULTS

4.1. Detection of Binary Candidates

From the different epochs' radial velocities we can check for the presence of variations with time. To quantify this, we follow the standard procedure of comparing the dispersion of the average radial velocity for each star with the average uncertainty in the determination of each radial velocity. This can be done by calculating the external-to-internal velocity dispersion ratio (σ_E/σ_I) as defined by Abt et al. (1972). Radial velocity variables can then be easily flagged out as they show σ_E/σ_I above 3, which is equivalent to saying that the variation in radial velocity is 3 σ above the expected uncertainties.

Binary motion is not the only source for scatter in the determination of radial velocities for a star. Stellar winds and atmospheric turbulence, both present in early type stars, also introduce apparent changes in the derivation of radial velocities at different epochs, but in these cases the internal errors are large too. A clear example of this is star #205 in the ionizing cluster of NGC 6611 (Bosch et al. 1999).

In addition to the results presented in Table 2, the high S/N of our spectra has also allowed us to detect several double-lined binaries that show evident variation of their absorption line profiles from epoch to epoch. Examples of these can be seen in Figures 1 and 2. Individual radial velocities are difficult to measure for these cases; therefore some of these stars are not included in Table 2. These 10 stars (including the four present in Table 2) are listed in Table 3.

An inspection of Table 2 shows that 17 out of 46 stars show radial velocity variations. If we add the stars present in Table 3 (excluding P613, which already shows radial velocity variations in Table 2), we have our complete set of binary star candidates, which rises to 25 out of 52 stars ($\sim$ 48%).

The mass ratio of binary components, orbital parameters, number of observations, and radial velocity accuracy can impact the statistics of detected binaries in star clusters. In an effort to quantify these effects, Bosch & Meza (2001) performed Monte Carlo simulations including all the parameters listed above. Feeding our GMOS data parameters into these simulations, we find that our detection rate is consistent with a population of 100% binaries.

4.2. Cluster Kinematics

After removing the confirmed and candidate binaries, the nonbinary population of our sample decreases to 26 stars, still enough to calculate a representative value of the stellar radial velocity dispersion (σ_r). In calculating it, we must keep in mind that each radial velocity measurement has its intrinsic error (σ_{int}), which must be subtracted quadratically from the observed (σ_{obs}) velocity dispersion. The former is the average

Table 2
Radial Velocities Determined for Sample Stars

Id	Sp. T	V_r	σ_I	V_r	σ_I	V_r	σ_I	V_r	σ_I	V_r	σ_I	V_r	σ_I	V_r	σ_I	$\frac{\sigma_{||}}{\langle\sigma_I\rangle}$
15 (I)	O8.5 V	299.1	5.5			272.7	9.0	207.5	4.9	289.3	5.7	255.2	5.6			5.9
32 (II)	O9 IV	283.3	6.3	271.6	4.2	261.1	4.8	271.3	4.3	278.3	4.3	275.5	4.1			1.6
124 (I)	O8.5 V	266.0	4.2	239.3	3.7	209.7	6.0	268.7	3.3	243.5	3.5	261.0	5.3			5.1
171 (I)	O8 V	272.7	3.7	286.5	5.4	256.9	5.0	258.7	4.7	276.7	6.1	269.2	7.1			2.1
260 (II)	B0.5: V	286.0	9.1	274.7	5.9	261.0	9.4	266.6	4.2	304.5	3.8	271.5	9.1	278.4	6.1	2.3
305 (II)	B0-B0.5 V	269.5	9.7	269.5	6.1	249.9	6.4	265.4	3.3	258.9	4.8	253.1	4.9	282.5	5.3	1.4
316 (I)	O6.5 IV	286.7	5.0	366.0	6.7	302.8	3.9	214.5	4.1	349.8	8.7	302.5	5.7			9.4
485 (II)	O8-9 V	277.3	5.3	260.1	5.5	255.7	8.1	278.7	3.5	251.2	5.5	259.8	6.2	269.1	4.0	2.0
531 (II)	O8 V	309.3	7.1	247.6	3.7	221.2	9.3	260.9	3.7	276.9	9.0	324.6	11.3	241.7	3.5	5.3
541 (I)	O7.5 V	239.2	6.2	276.0	7.0	272.4	3.4	232.8	3.9	358.5	6.2	232.1	3.9			9.4
613 (II)	O8.5 V	246.2	4.1	275.6	4.8	332.9	9.1	257.6	3.8	264.5	4.4	245.9	7.5	236.3	5.5	5.8
649 (II)	O8-9 V	282.6	9.1	286.3	6.5	280.2	6.4	276.9	3.7	281.5	6.7	285.2	5.9	280.1	4.0	0.5
684 (II)	B0: I	275.7	7.9	270.4	5.4	247.8	7.8	252.7	3.4	254.8	5.0	272.5	8.7	270.7	6.4	1.9
713 (I)	O5 V	238.3	4.7	316.1	6.9	298.8	4.4	320.4	5.3	297.0	7.2	312.6	10.9			4.6
716 (II)	O5.5 III(f)	274.0	3.6	273.8	7.4	266.1	4.6	271.4	3.8	275.3	4.4	279.8	4.1	277.5	3.8	1.0
747 (I)	O6-8 V	182.4	3.8	213.9	5.6	306.5	5.0	331.0	4.0	248.3	9.2	306.0	7.5			10.1
809 (II)	O8-9 V	263.8	9.4	268.7	5.5	256.0	7.9	279.3	3.8	265.2	4.0	257.6	11.7	269.1	6.1	1.2
871 (II)	O4 V((f*))	275.2	7.5	272.8	6.3	268.7	8.4	281.3	3.6	282.2	8.3	289.1	4.2	278.2	8.2	1.2
885 (II)	O5 III	276.1	5.1	289.1	4.1	286.3	7.6	234.8	3.2	270.5	8.1	267.2	5.3	283.5	4.8	3.5
905 (I)	O9-B0 V	268.5	6.9	267.4	8.2	271.2	11.1	257.5	4.1	261.9	5.1	265.5	5.8			0.7
956 (I)	B1-2 V	268.4	6.6	284.5	6.4	239.1	3.7	265.7	6.5	270.3	7.1	274.3	6.8			2.5
975 (II)	O6-7 V((f))	297.4	4.2	288.8	3.7	266.7	6.5	281.1	3.6	289.2	8.9	282.9	6.0	287.2	3.8	1.9
1022 (I)	O5: V	274.3	4.5	288.9	4.9	271.1	5.0	290.0	5.4	278.4	8.2	279.5	6.6			1.3
1035 (II)	O3-6 V	287.8	11.2	278.1	7.6	263.5	8.4	277.7	4.2	273.6	4.9	285.1	3.4	281.3	4.7	1.3
1063 (II)	O6-7 V	269.5	6.6	265.3	3.7	265.9	8.9	261.6	4.1	272.3	4.2	256.5	7.2	266.4	4.9	1.0
1109 (I)	O9 V	274.2	5.7	293.9	8.6	278.6	4.5	278.5	3.6	253.0	4.4	248.5	8.1			3.0
1139 (I)	Bo V	256.3	5.4	266.2	8.0	259.1	4.1	269.4	4.2	257.1	5.5	271.7	5.4			1.2
1163 (I)	O4 If*	263.6	5.5	273.3	7.9	259.5	4.8	265.5	8.1	266.5	11.9	260.9	13.0			0.6
1218 (II)	O6: V	294.1	3.4	283.6	4.1	273.0	7.1	287.4	3.8	281.4	3.6	297.7	10.3	294.3	4.5	1.7
1222 (I)	O3-6 V	277.8	4.7	272.7	5.9	258.2	4.8	263.4	6.0	272.3	8.4	265.9	4.6			1.3
1247 (I)	B0.5 IV	248.7	8.8	263.2	4.3	248.1	15.3	243.5	9.1	269.7	8.4	273.3	4.4			1.5
1260 (I)	O3 V	289.0	5.0	294.8	5.1	279.3	5.0	294.5	4.2	291.4	9.4	297.3	5.9			1.1
1339 (I)	B0-0.2 IV	252.7	6.1	271.8	5.2	255.0	6.3	260.8	4.8	261.0	7.1	273.7	6.6			1.4
1341 (I)	O3-4 III(f*)	287.9	7.6	300.3	6.0	301.2	4.4	305.3	5.2	267.2	12.6	304.5	13.9			1.8
1350 (II)	O6 III(f*)	266.1	4.7	269.3	7.5	255.9	6.9	267.1	3.8	261.7	6.5	271.6	8.9	253.0	6.1	0.9
1401 (I)	O8 V	248.2	3.1	260.7	3.6	279.7	5.2	282.6	4.5	321.2	10.9	237.5	6.7			5.3
1468 (II)	O9.5 V	268.2	9.5	276.1	5.7	259.9	4.4	262.7	4.3	263.0	5.8	264.1	8.4	274.1	5.9	0.9
1531 (I)	O6.5 V((f))	276.1	4.5	304.0	5.6	290.9	3.5	295.2	4.0	291.0	8.1	299.8	5.6			1.9
1553 (I)	O7 V	267.1	4.2	241.0	6.0	230.2	7.8	287.4	3.4	309.7	6.5	316.2	6.8			6.1
1584 (II)	B0-1 V			281.7	5.9	250.7	6.9	277.2	4.0	299.0	7.2	283.1	36.3	293.8	6.1	1.5
1604 (I)	B1 V	270.9	5.8	261.3	7.6	251.0	4.0	269.4	4.1	337.1	16.2	326.7	27.3			3.4
1607 (II)	O7: If	281.7	3.6	279.7	4.7	267.2	3.7	271.8	3.9	269.1	4.5	277.9	4.1	274.4	4.7	1.5
1614 (I)	O5-6 V((f))	274.0	3.1	293.7	4.4	276.9	5.9	286.8	3.8	280.2	8.3	291.3	5.6			1.5
1619 (I)	O8 III(f)	267.9	3.2	321.7	5.1	301.5	3.3	292.9	4.2	305.7	10.3	291.0	5.5			3.4
1729 (II)	B1 II-III	281.3	8.5	270.8	4.6	194.2	6.4	233.2	6.4	209.2	11.5	211.0	3.6	286.1	5.2	5.2
1840 (II)	B1 V	262.4	8.2	270.8	4.3	273.5	5.8	245.1	5.5	271.4	3.2	251.3	5.3	296.9	5.9	2.2
1969 (I)	B0.7 IV	273.3	5.1	276.9	6.5	285.0	4.1	299.6	4.1	312.0	5.2	313.2	6.6			3.3
1988 (I)	B0.5 V	218.3	5.3	325.2	6.2	234.5	3.6	263.0	3.3	204.2	5.6	311.6	8.0			9.3

Notes. Stellar identifications by Parker (1993) are in Column 1 and Spectral types from Bosch et al. (1999a) are included in Column 2. Columns 3 through 16 include radial velocities and uncertanties (all in km s^{-1}) for each epoch of observation. Column 17 lists the ratio between epoch-to-epoch variations and the average uncertainties.

of the $\langle\sigma_I\rangle$ values over the whole sample of nonradial velocity variable stars, while the latter is directly derived as the standard deviation around the average radial velocity derived for the same subset of stars in the cluster and it therefore follows that $\sigma_r{}^2 = \sigma_{obs}{}^2 - \langle\sigma_{int}\rangle^2$. For our sample, $\sigma_{obs} = 10.3$ km s^{-1}, $\langle\sigma_{int}\rangle = 6.2$ km s^{-1}, which yield a value of 8.3 km s^{-1} for the actual radial velocity dispersion. This seems to confirm the suggestion by Bosch et al. (2001) based on simulations that the large values derived for the stellar velocity dispersion were most probably due to the presence of binaries. As expected, if we derive the radial velocity dispersion from an individual GMOS mask observation for a single epoch, we find values as high as 30 km s^{-1}, consistent with what was previously found in Bosch et al. (2001) from single-epoch NTT data.

This is the first time that a radial velocity dispersion is found for massive stars in NGC 2070, free from contamination by the motion of binary stars. We can therefore safely proceed to compare it with the stellar kinematics expected for 30 Dor in order to check if the cluster is virialized. Following the estimations for the photometric mass derived in Selman et al. (1999), we find that the stellar mass within the volume covered by our spectroscopic survey is about 4.5×10^5 $M_\odot$. If the
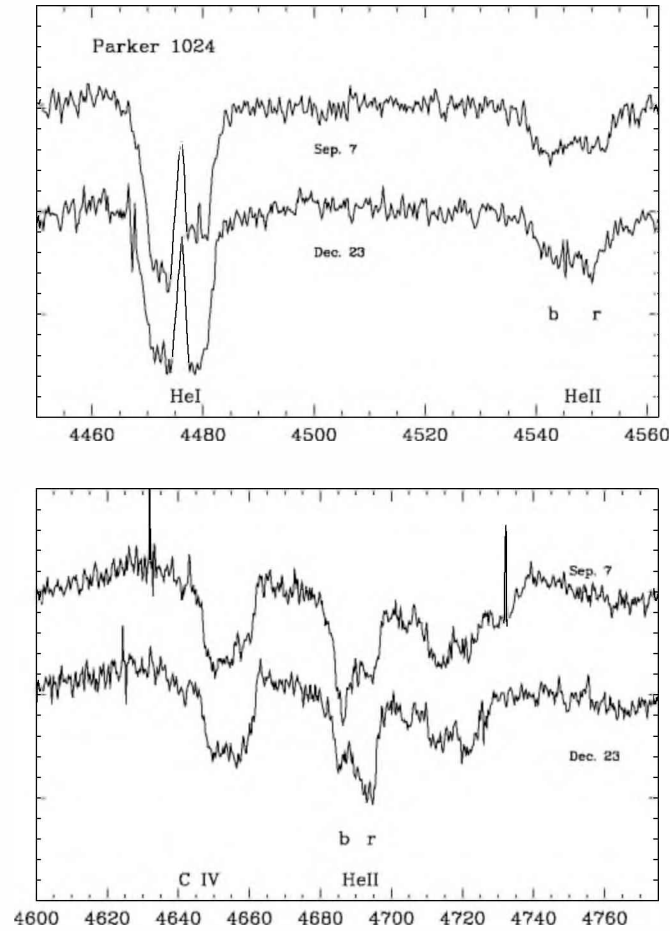
Figure 1. Spectra obtained for Parker 1024 on two different epochs, showing the variation of observed profiles for selected absorption lines. Both spectra are continuum normalized but shifted in the y-axis by 0.05 continuum units for comparison purposes and identified by their respective observing date during 2005. Relevant absorption profiles are labeled and double troughs are identified indicating their blue (b) and red (r) components. Note the evident changes in the relative intensities of the blue and red troughs, particularly for He II 4542 Å and He II 4686 Å, suggesting that the binary pair was observed on opposite orbital phases.

Table 3
Stars with Evidence of Binarity from Individual Spectra

ID	Comment
260	Asymmetrical on 19/12
613	He II lines look double on 24/12
674	Double lines on 22/12 & 24/12
805	Double lined on 23/12
955	Looks double on 20/12 & 23/12
956	Looks Asymmetrical on 23/12
1024	Double profile on three epochs
1031	Double lined on 07/09 & 20/12
1035	He I lines look broad on 24/12
1938	Broad lines on 22/12

Notes. Stellar identifications by Parker (1993) are shown in Column 1. Column 2 describes the characteristics found among spectral features that suggest binary nature.

stellar velocity distribution is isotropic, we can follow Binney & Tremaine (1987) and estimate the expected radial velocity dispersion as

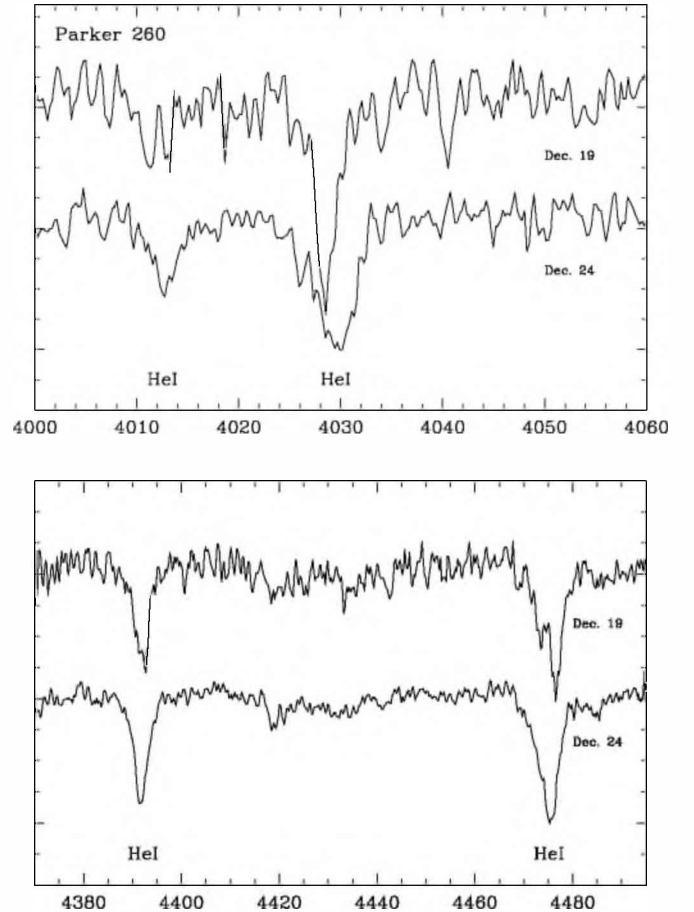$$\sigma_r^2 = \frac{4.5 \times 10^{-3} M}{3 R_c},$$

Figure 2. Same as Figure 1, for Parker 260 with a 0.2 continuum units shift between spectra. In this case the profile variations show changes from a well-behaved absorption profile (2005 December 24) to an asymmetrical profile (2005 December 19). These changes are particularly evident for the He I 4387 Å and 4026 Å profiles. Although the most evident changes are seen as a double peaked profile in He I 4471 Å the presence of nebular emission contamination in this line cannot be ruled out.

where masses are in $M_\odot$, distances in pc, and σ in km s^{-1}. The velocity dispersion derived for the total mass of 30 Dor, for a half-mass radius of 14 pc, is about 8 km s^{-1}. Our derived value of 8.3 km s^{-1} is well within the observational and sampling uncertainties. If there are more binaries yet to be discovered a slight reduction in the observed value is expected (although it is unlikely that they would show such large radial velocity variations that would dramatically enhance the current value).

Another interesting issue is that the single-star population does not confirm the evidence toward mass segregation that was suggested in Bosch et al. (2001), at least for the massive stars. However, the fact that massive stars seem to have a relatively low velocity dispersion cannot rule out dynamical mass segregation with low-mass stars.

5. CONCLUSIONS

Based on seven epoch observations with the GMOS in Gemini South, we have presented observational evidence that shows that the binary fraction among massive stars in NGC 2070 may be very high. Indeed we already detect a 50% binary candidacy with only three epoch observations, which suggests that it is only a lower limit. The evidence pointing toward a high binarity fraction has an important effect on the massive end of the stellar cluster IMF, and should not be overlooked.

If a high binary fraction is common among massive young clusters, virial masses obtained from the observed global velocity dispersions in unresolved young clusters might be overestimated by a large factor, as discussed in Kouwenhoven & de Grijs (2008).

Regardless of the origin of the stellar radial velocity variability, the analysis of the nonvariable subset provides an important result regarding the kinematics of the stellar cluster itself. The radial velocity dispersion determined for the 30 Doradus ionizing cluster agrees, within observational errors, with the stellar kinematics expected if the cluster is virialized and its total mass is derived from the photometric plus ionized gas masses. This suggests that the stellar cluster is far from disruption and stands as a firm candidate for a future globular cluster system.

More observations in further epochs should allow us to confirm the binary nature of radial velocity variables detected in this work and derive the orbital parameters and individual masses of members of the binary pairs. The success of the GMOS in the MOS mode makes it a very efficient tool for discovering massive binaries in large numbers using a relatively small amount of telescope time.

REFERENCES

Abt, H. A., Levy, S. G., & Gandet, T. L. 1972, AJ, 77, 138
Binney, J., & Tremaine, S. 1987, Galactic Dynamics (Princeton, NJ: Princeton Univ. Press), 747
Bosch, G. 1999, PhD thesis, Cambridge Univ.
Bosch, G., & Meza, A. 2001, RevMexAA, 27, 29
Bosch, G. L., Morrell, N. I., & Niemela, V. S. 1999, RevMexAA, 35, 85
Bosch, G., Selman, F., Melnick, J., & Terlevich, R. 2001, A&A, 380, 137
Bosch, G., Terlevich, R., Melnick, J., & Selman, F. 1999, A&AS, 137, 21
Kouwenhoven, M. B. N., & de Grijs, R. 2008, A&A, 480, 103
Lada, C. J. 2006, ApJ, 640, L63
Mason, B. D., Gies, D. R., Hartkopf, W. I., Bagnuolo, W. G., Jr., ten Brummelaar, T., & McAlister, H. A. 1998, AJ, 115, 821
Parker, J. W. 1993, AJ, 106, 560
Sana, H., Gosset, E., Nazé, Y., Rauw, G., & Linder, N. 2008, MNRAS, 386, 447
Selman, F., Melnick, J., Bosch, G., & Terlevich, R. 1999, A&A, 347, 532